

Moments of Structure Functions in Full QCD*

D. Dolgov, R. Brower, S. Capitani, J. W. Negele, A. Pochinsky, D. Renner

Center for Theoretical Physics, MIT, 77 Massachusetts Ave., Cambridge, MA 02139, USA

N. Eicker, T. Lippert, K. Schilling

Department of Physics, University of Wuppertal, D-42097 Wuppertal, Germany

R. G. Edwards,^a U. M. Heller^b

^aJefferson Lab, 12000 Jefferson Avenue, MS 12H2, Newport News, Virginia 23606, USA

^bCSIT, Florida State University, Tallahassee FL 32306 USA

Moments of the quark density distribution, moments of the quark helicity distribution, and the tensor charge are calculated in full QCD. Calculations of matrix elements of operators from the operator product expansion have been performed on $16^3 \times 32$ lattices for Wilson fermions at $\beta = 5.6$ using configurations from the SESAM collaboration and at $\beta = 5.5$ using configurations from SCRI. One-loop perturbative renormalization corrections are included. Selected results are compared with corresponding quenched calculations and with calculations using cooled configurations.

1. INTRODUCTION

Given the detailed experimental knowledge of the light cone distributions of quarks and gluons in the nucleon, it is of interest to use lattice QCD both to calculate the quark and gluon structure of the nucleon from first principles and to reveal the underlying mechanisms giving rise to this structure. Using the operator product expansion, it is possible to calculate moments of quark distributions, and we report here the first calculations in full QCD [1]. We also compare full QCD results with quenched QCD and with configurations that have been cooled to remove all the gluon contributions except for those of instantons.

2. DEFINITIONS

The moments of the spin-independent structure functions $F_1(x, Q^2)$, $F_2(x, Q^2)$ and the spin-dependent structure functions $g_1(x, Q^2)$, $g_2(x, Q^2)$ are related to products of Wilson coefficients $C_n(Q^2/\mu^2)$ times hadronic matrix elements:

$$\begin{aligned} \int_0^1 dx x^n F_1(x, Q^2) &= \frac{1}{2} C_{n+1}^v \left(\frac{Q^2}{\mu^2}\right) \langle x^n q \rangle(\mu) \\ \int_0^1 dx x^n F_2(x, Q^2) &= C_{n+2}^v \left(\frac{Q^2}{\mu^2}\right) \langle x^{n+1} q \rangle(\mu) \\ \int_0^1 dx x^n g_1(x, Q^2) &= \frac{1}{4} C_n^a \left(\frac{Q^2}{\mu^2}\right) 2 \langle x^n \Delta q \rangle(\mu) \\ \int_0^1 dx x^n g_2(x, Q^2) &= \frac{1}{4} \frac{n}{n+1} \left[C_n^d \left(\frac{Q^2}{\mu^2}\right) d_n(\mu) \right. \\ &\quad \left. - C_n^a \left(\frac{Q^2}{\mu^2}\right) 2 \langle x^n \Delta q \rangle \right]. \end{aligned}$$

These matrix elements, denoted $\langle x^n q \rangle$ (which equals $v_{n+1}^{(q)}$ in the notation of ref.[2]), $\langle x^n \Delta q \rangle$ (which equals $\frac{1}{2} a_n^{(q)}$ [2]) and d , as well as the moments of the transversity distribution $h(x, Q^2)$, $\langle x^n \delta q \rangle$, are related to expectation values of the following operators in the proton ground state:

$$\begin{aligned} 2 \langle x^{n-1} q \rangle P_{\mu_1} \cdots P_{\mu_n} &= \frac{1}{2} \langle PS | \left(\frac{i}{2}\right)^{n-1} \bar{\psi} \gamma_{\{\mu_1} \overleftrightarrow{D}_{\mu_2} \cdots \overleftrightarrow{D}_{\mu_n} \} \psi | PS \rangle \\ \frac{2}{n} \langle x^n \Delta q \rangle S_{\{\sigma} P_{\mu_1} \cdots P_{\mu_n\}} &= - \langle PS | \left(\frac{i}{2}\right)^n \bar{\psi} \gamma_5 \gamma_{\{\sigma} \overleftrightarrow{D}_{\mu_1} \cdots \overleftrightarrow{D}_{\mu_n} \} \psi | PS \rangle \\ \frac{1}{n} d_n S_{[\sigma} P_{\{\mu_1} \cdots P_{\mu_n\}} &= - \langle PS | \left(\frac{i}{2}\right)^n \bar{\psi} \gamma_5 \gamma_{[\sigma} \overleftrightarrow{D}_{\{\mu_1} \cdots \overleftrightarrow{D}_{\mu_n} \} \psi | PS \rangle \\ \frac{1}{m_N} \langle x^n \delta q \rangle S_{[\mu} P_{\{\nu} P_{\mu_1} \cdots P_{\mu_n\}} &= \langle PS | \left(\frac{i}{2}\right)^n \bar{\psi} \gamma_5 \sigma_{\mu\{\nu} \overleftrightarrow{D}_{\mu_1} \cdots \overleftrightarrow{D}_{\mu_n} \} \psi | PS \rangle. \end{aligned}$$

In the parton model, these matrix elements correspond to the following moments of quark longi-

*Talk presented by J. W. Negele. Work supported in part by the U.S. Department of Energy (DOE) under cooperative research agreement # DE-FC02-94ER 40818.

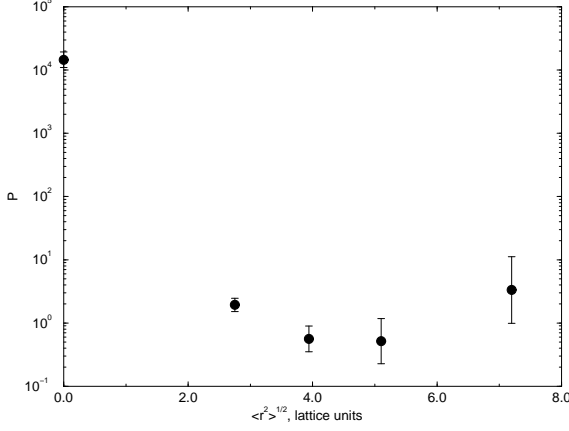


Figure 1. Contamination by excited states, P , as a function of the source RMS radius

tudinal and transverse distributions:

$$\begin{aligned} x^n q &\equiv \int_0^1 dx x^n (q_{\downarrow}(x) + q_{\uparrow}(x)) \\ x^n \Delta q &\equiv \int_0^1 dx x^n (q_{\downarrow}(x) - q_{\uparrow}(x)) \\ x^n \delta q &\equiv \int_0^1 dx x^n (q_{\top}(x) - q_{\perp}(x)). \end{aligned}$$

3. SOURCES

Connected diagrams are calculated using sequential propagators generated by the upper two components of the nucleon source $J^\alpha = u_a^\alpha u_b^\beta (C\gamma_5)_{\beta,\beta'} d_c^{\beta'} \epsilon^{abc}$. The overlap with the physical proton ground state was optimized using Wuppertal smearing [3] to minimize the contamination $P = \sum_{n \neq 0} |\langle J|n\rangle|^2 / |\langle J|0\rangle|^2$. Figure 1 shows that varying the smearing reduced P by over 4 orders of magnitude, yielding an overlap with the physical ground state of approximately 70%. Dirichlet boundary conditions were used for quarks in the t-direction.

4. OPERATORS AND PERTURBATIVE RENORMALIZATION

The continuum operators defined above are approximated on a discrete cartesian lattice using representations of the hypercubic group that eliminate operator mixing where possible and minimize the number of non-zero components of

Table 1

Operators used to measure moments of quark distributions

	H(4) mix	\vec{p}	lattice operator
$xq_c^{(a)}$	$\mathbf{6}_3^+$ no	$\neq 0$	$\bar{q}\gamma_{\{1}\overleftrightarrow{D}_4\}q$
$xq_c^{(b)}$	$\mathbf{3}_1^+$ no	0	$\bar{q}\gamma_4\overleftrightarrow{D}_4q$ $-\frac{1}{3}\sum_{i=1}^3\bar{q}\gamma_i\overleftrightarrow{D}_i q$
x^2q_c	$\mathbf{8}_1^-$ yes	$\neq 0$	$\bar{q}\gamma_{\{1}D_1\overleftrightarrow{D}_4\}q$ $-\frac{1}{2}\sum_{i=2}^3\bar{q}\gamma_{\{i}\overleftrightarrow{D}_i\overleftrightarrow{D}_4\}q$
x^3q_c	$\mathbf{2}_1^+$ no*	$\neq 0$	$\bar{q}\gamma_{\{1}\overleftrightarrow{D}_1\overleftrightarrow{D}_4\overleftrightarrow{D}_4\}q$ $+ \bar{q}\gamma_{\{2}\overleftrightarrow{D}_2\overleftrightarrow{D}_3\overleftrightarrow{D}_3\}q$ $-(3 \leftrightarrow 4)$
Δq_c	$\mathbf{4}_4^+$ no	0	$\bar{q}\gamma^5\gamma_3q$
$x\Delta q_c^{(a)}$	$\mathbf{6}_3^-$ no	$\neq 0$	$\bar{q}\gamma^5\gamma_{\{1}\overleftrightarrow{D}_3\}q$
$x\Delta q_c^{(b)}$	$\mathbf{6}_3^-$ no	0	$\bar{q}\gamma^5\gamma_{\{3}\overleftrightarrow{D}_4\}q$
$x^2\Delta q_c$	$\mathbf{4}_2^+$ no	$\neq 0$	$\bar{q}\gamma^5\gamma_{\{1}\overleftrightarrow{D}_3\overleftrightarrow{D}_4\}q$
δq_c	$\mathbf{6}_1^+$ no	0	$\bar{q}\gamma^5\sigma_{34}q$
$x\delta q_c$	$\mathbf{8}_1^-$ no	$\neq 0$	$\bar{q}\gamma^5\sigma_3\{\overleftrightarrow{D}_1\}q$
d_1	$\mathbf{6}_1^+$ no**	0	$\bar{q}\gamma^5\gamma_{\{3}\overleftrightarrow{D}_4\}q$
d_2	$\mathbf{8}_1^-$ no**	$\neq 0$	$\bar{q}\gamma^5\gamma_{\{1}\overleftrightarrow{D}_3\overleftrightarrow{D}_4\}q$

Table 2

Perturbative renormalization constants

	γ	B^{LATT}	B^{MS}	Z	
				$\beta=6.0$	$\beta=5.6$
$xq^{(a)}$	$\frac{8}{3}$	-3.16486	$-\frac{40}{9}$	0.989	0.988
$xq^{(b)}$	$\frac{8}{3}$	-1.88259	$-\frac{40}{9}$	0.978	0.977
x^2q	$\frac{25}{6}$	-19.57184	$-\frac{67}{9}$	1.102	1.110
x^3q	$\frac{157}{30}$	-35.35192	$-\frac{2216}{225}$	1.215	1.231
Δq	0	15.79628	0	0.867	0.857
$x\Delta q^{(a)}$	$\frac{8}{3}$	-4.09933	$-\frac{40}{9}$	0.997	0.997
$x\Delta q^{(b)}$	$\frac{8}{3}$	-4.09933	$-\frac{40}{9}$	0.997	0.997
$x^2\Delta q$	$\frac{25}{6}$	-19.56159	$-\frac{67}{9}$	1.102	1.110
δq	1	16.01808	-1	0.856	0.846
$x\delta q$	3	-4.47754	-5	0.996	0.995
d_1	0	0.36500	0	0.997	0.997
d_2	$\frac{7}{6}$	-15.67745	$-\frac{35}{18}$	1.116	1.124

the nucleon momentum. The operators we have used are shown in Table 1, where we have indicated whether the spatial momentum components

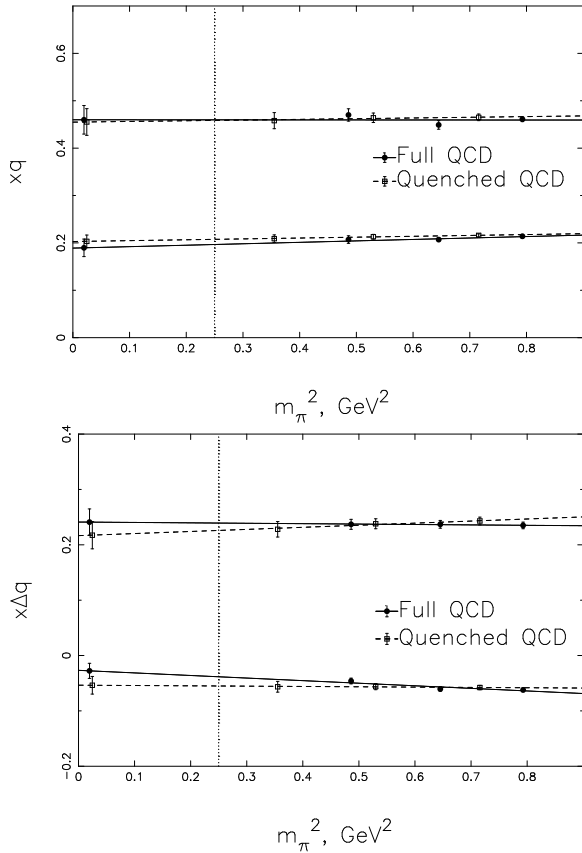


Figure 2. Comparison of chiral extrapolations of full and quenched calculations of $\langle xq \rangle$ and $\langle x\Delta q \rangle$ showing agreement within statistical errors

are non-zero and whether mixing occurs. (Note, no* indicates a case in which mixing could exist in general but vanishes perturbatively for Wilson or overlap fermions and no** indicates perturbative mixing with *lower* dimension operators for Wilson fermions but no mixing for overlap fermions.)

The perturbative renormalization coefficients we have calculated and used in this work are tabulated in Table 2 [4]. The factor to convert lattice results to the continuum \overline{MS} scheme is $Z(g_0^2 = 6/\beta) = 1 - \frac{g_0^2}{16\pi^2} \frac{4}{3} (B^{LATT} - B^{\overline{MS}})$.

5. RESULTS

The moments listed in Table 1 were calculated [1] on $16^3 \times 32$ lattices for Wilson fermions in

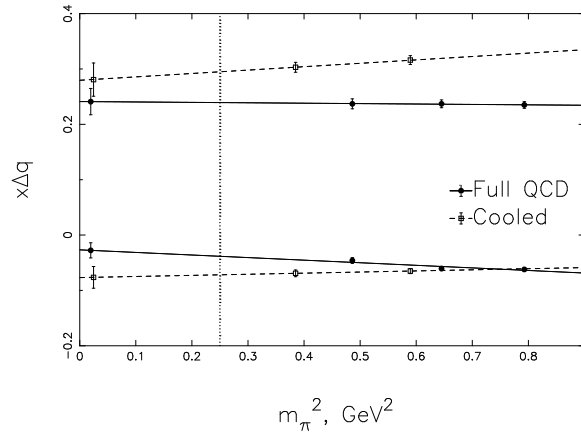


Figure 3. Comparison of chiral extrapolations of full and cooled calculations of $\langle x\Delta q \rangle$ showing the extent to which instantons reproduce the full result

full QCD at $\beta = 5.6$ using 200 SESAM configurations at each of 4 $\kappa's$ and at $\beta = 5.5$ using 100 SCRI configurations at 3 $\kappa's$. They were also calculated with two sets of 100 full QCD configurations cooled with 50 cooling steps and in quenched QCD at $\beta = 6.0$ using 200 configurations at each of 3 $\kappa's$. Typical chiral extrapolations for operators calculated with nucleon momentum equal to zero are shown in Figure 2 for full and quenched calculations of $\langle xq \rangle$ and $\langle x\Delta q \rangle$, showing agreement within statistical errors. To avoid finite volume errors at the lightest quark mass, the SESAM [5] results were extrapolated using the three heaviest quark masses. Table 3 shows a major result of our work, that there is complete agreement within statistics between full and quenched results. Statistics with the SCRI configurations [6] are not yet adequate to present extrapolations in the coupling constant.

Typical chiral extrapolations for cooled configurations are compared with the corresponding uncooled full QCD calculations in Figure 3. This qualitative agreement between cooled and uncooled results occurs at light quark mass for all the twist-2 matrix elements we calculated and demonstrates the degree to which the instanton content of the configurations and their associated zero modes dominate light hadron structure [7].

Table 3

Comparison of our full QCD and quenched results with other lattice calculations and phenomenology at 4 GeV in \overline{MS}

	QCDSF	QCDSF ($a = 0$)	Wuppertal	Quenched	Full QCD (3 pts)	Phenomenology (q_{val})
xu_c	0.452(26)			0.454(29)	0.459(29)	0.284
xd_c	0.189(12)			0.203(14)	0.190(17)	0.104
$xu_c - xd_c$	0.263(17)			0.251(18)	0.269(23)	0.180
x^2u_c	0.104(20)			0.119(61)	0.176(63)	0.083
x^2d_c	0.037(10)			0.029(32)	0.0314(303)	0.025
x^3u_c	0.022(11)			0.037(36)	0.0685(392)	0.032
x^3d_c	-0.001(7)			0.009(18)	-0.00989(1529)	0.008
Δu_c	0.830(70)	0.889(29)	0.816(20)	0.888(80)	0.860(69)	0.918
Δd_c	-0.244(22)	-0.236(27)	-0.237(9)	-0.241(58)	-0.171(43)	-0.339
$\Delta u_c - \Delta d_c$	1.074(90)	1.14(3)	1.053(27)	1.129(98)	1.031(81)	1.257
$x\Delta u_c$	0.198(8)			0.215(25)	0.242(22)	0.150
$x\Delta d_c$	-0.048(3)			-0.054(16)	-0.0290(129)	-0.055
$x^2\Delta u_c$	0.087(14)			0.027(60)	0.116(42)	0.050
$x^2\Delta d_c$	-0.025(6)			-0.003(25)	0.00142(2515)	0.016
δu_c	0.93(3)	0.980(30)		1.01(8)	0.963(59)	
δd_c	-0.20(2)	-0.234(17)		-0.20(5)	-0.202(36)	
d_2^u	-0.206(18)			-0.233(86)	-0.228(81)	
d_2^d	-0.035(6)			0.040(31)	0.0765(310)	

Comparison in Table 3 of our quenched results with those of the QCDSF collaboration [2] and the full QCD results with those of Wuppertal [5] shows complete consistency. Since the phenomenological quantity q_{val} [8] does not correspond precisely to the connected diagrams we calculate, the most meaningful comparison is with $u - d$ differences. The two most physically significant discrepancies arising from this table are the fact that the difference in first moment is $\sim 0.25 - 0.29$ on the lattice and 0.18 experimentally and the axial charge is $\sim 1.0 - 1.1$ on the lattice and 1.26 experimentally. We have clearly shown that these discrepancies do not arise from quenching and believe both indicate inadequate treatment of the pion cloud of the nucleon due to the small physical volume and heavy quark mass.

REFERENCES

1. D. Dolgov, Ph.D. dissertation, MIT (2000).
2. M. Göckeler *et al.*, Phys. Rev. D53 (1996) 2317; Phys. Lett. B414 (1997) 340; hep-ph/9711245; hep-ph/9909253; C. Best *et al.*, hep-ph/9706502; S. Capitani *et al.*, Nucl. Phys. (Proc. Suppl.) B79 (1999) 548.
3. C. Alexandrou *et al.*, Phys. Lett. B256 (1991) 60; C. R. Allton *et al.*, Phys. Rev. D47 (1993) 5128.
4. S. Capitani and G. Rossi, Nucl. Phys. B433 (1995) 351; G. Beccarini *et al.*, Nucl. Phys. B456 (1995) 271; M. Göckeler *et al.* Nucl. Phys. B472 (1996) 309; S. Capitani *et al.*, hep-lat/0007004; S. Capitani, hep-lat/0005008; hep-lat/0009018.
5. N. Eicker *et al.*, Phys. Rev. D59 (1999) 014509; S. Güsken *et al.*, Phys. Rev. D59 (1999) 054504; hep-lat/9901009.
6. K. M. Bitar *et al.* Phys. Rev. D54, (1996) 3546.
7. M. -C. Chu *et al.*, Phys. Rev. D49 (1994) 6039; T. L. Ivanenko and J. W. Negele, Nucl. Phys. (Proc. Suppl.) B63 (1998) 504; D. Dolgov *et al.*, Nucl. Phys. (Proc. Suppl.) B73 (1999) 300.
8. T. Gehrman and W. J. Stirling, Phys. Rev. D53 (1996) 6100.

